

Luminescence Spectra of Single Crystals of $\text{Cs}_2\text{ZrCl}_6:\text{UO}_2\text{Cl}_4^{2-}$ at Low Temperatures. Vibronic Structure of UO_2^{2+} Doped in a Cubic Host

David H. Metcalf,* Sheng Dai,* G. D. Del Cul, and L. M. Toth

Chemical Technology Division, Oak Ridge National Laboratory, Oak Ridge, Tennessee 37831-6181

Received January 27, 1995[⊗]

Low-temperature (20 K–120 K) high-resolution luminescence spectra of $\text{UO}_2\text{Cl}_4^{2-}$ doped in cubic crystals of Cs_2ZrCl_6 are reported. The luminescence is associated with the $A_{1g} \leftarrow E_g$ electronic origin transition and vibronic transitions associated with this origin. The vibronic structure is consistent with the $\text{UO}_2\text{Cl}_4^{2-}$ ion having D_{4h} symmetry. The distribution of intensity among members of vibronic progressions associated with the UO_2^{2+} stretching frequency was used to determine Huang–Rhys parameters for both the ground (A_{1g}) and excited (E_g) states. The parameters are consistent with a difference of U–O bond length of ca. 7 pm between the ground and excited states. The energy of the electronic origin transition is less than that of the neat $\text{Cs}_2\text{UO}_2\text{Cl}_4$ crystal [Denning, R. G.; Snellgrove, T. R.; Woodward, D. R. *Mol. Phys.* **1976**, *32*, 419–442] by some 400 cm^{-1} . This is explained by structural and Coulombic effects on the $\text{UO}_2\text{Cl}_4^{2-}$ ion as it is accommodated in the Cs_2ZrCl_6 lattice.

Introduction

Low-temperature absorption and luminescence of the uranyl ion have been of interest since the time of the Manhattan Project, when the spectra of a large number of crystalline uranyl systems were measured at liquid hydrogen temperatures.¹ Luminescence spectra of these compounds are marked by the appearance of many sharp vibronic lines based on a common origin. Absorption spectra are likewise marked by sharp vibronic lines based on multiple origin lines, which correspond to transitions from the ground state to different excited states. Few reports have appeared on the spectroscopy of uranyl ion doped into single crystals. Herein, we report single-crystal luminescence spectra of UO_2^{2+} ion doped into the cubic host Cs_2ZrCl_6 . Our analysis of the absorption spectra of this system will follow at a later date.

The crystal structure of Cs_2ZrCl_6 is cubic, space group $Fm\bar{3}m$, which is the hexachloroplatinate structure.² There are four ZrCl_6^{2-} ions per unit cell, and they occupy the corner and face-centered positions of the cubic unit cell. Each ZrCl_6^{2-} ion has exact O_h symmetry. There are eight cesium cations in each unit cell, and they are arranged at the corners of a cube, one half the length of the unit cell, that is centered within the unit cell. Cs_2ZrCl_6 is one member of an extensive isomorphous series, in which (with some exceptions) the cation can be replaced with NH_4^+ , K^+ , Rb^+ , Cs^+ , or TI^+ and the complex anion by HfCl_6^{2-} , TiCl_6^{2-} , SeCl_6^{2-} , SnCl_6^{2-} , TeCl_6^{2-} , PtCl_6^{2-} , PbCl_6^{2-} , ZrBr_6^{2-} , HfBr_6^{2-} , or SnBr_6^{2-} . For Cs_2ZrCl_6 , the unit cell length is 1041 pm,² and the closest Zr–Zr distance is 736 pm.

Crystals of Cs_2ZrCl_6 doped with UO_2^{2+} are easily grown from melts of ZrCl_4 and CsCl (in a 1:2 mole ratio) with added $\text{Cs}_2\text{UO}_2\text{Cl}_4$. The crystals used in the present study have about 1 mol % of U, compared to Zr. Crystals of Cs_2ZrCl_6 have been used previously as host materials for U^{4+} , in which UCl_6^{2-} ions occupy ZrCl_6^{2-} sites.³ In the present crystal, we assume that the uranyl ions also occupy ZrCl_6^{2-} sites and that each is further

complexed to four chloride ions, lowering the UO_2^{2+} symmetry to D_{4h} . The C_4 axis of each of the $\text{UO}_2\text{Cl}_4^{2-}$ ions is oriented along one of the three crystallographic axes, in a random fashion. Thus, polarized absorption spectra will not be productive in this isotropic system, although it may be possible to use polarized excitation–emission experiments to measure transition polarization ratios.

Denning and co-workers^{4,5} have studied the absorption of the $\text{UO}_2\text{Cl}_4^{2-}$ chromophoric unit as it exists in the neat crystal $\text{Cs}_2\text{UO}_2\text{Cl}_4$, and Flint and Tanner⁶ have reported the luminescence of this same system. This crystal is monoclinic, having space group $C2/m$.⁷ The uranyl axes are all oriented along one direction within the crystal, which is defined to be the molecular z -axis. This axis bisects the angle formed between the crystallographic a and c axes (the nonorthogonal axes in this crystal system), and is perpendicular to the crystallographic b -axis. Each $\text{UO}_2\text{Cl}_4^{2-}$ unit has exact C_{2h} symmetry, but is only slightly distorted from D_{4h} symmetry. Denning used low-temperature (4.2 K) polarized single-crystal absorption spectroscopy to locate and assign 12 origin transitions within the 20 000–28 000 cm^{-1} energy range.⁴ His assignments were based on effective D_{4h} symmetry for the uranyl ion, slightly distorted to D_{2h} symmetry. The ground state of UO_2^{2+} has the symmetry label Σ_g^+ in the $D_{\infty h}$ point group (the symmetry of “free” UO_2^{2+}), which transforms as A_{1g} in the D_{4h} point group or A_g in the D_{2h} point group. The first excited state, which serves as the origin for the luminescence observed for this system, has Π_g symmetry in the $D_{\infty h}$ point group, which transforms as E_g symmetry in the D_{4h} point group. It is split into B_{2g} and B_{3g} components in the D_{2h} point group, which, in Denning’s spectra, are separated by 1.6 cm^{-1} . These components are located at 20 095.7 and 20 097.3 cm^{-1} .

None of the absorptive origin transitions directly observed by Denning are allowed by an electric-dipole mechanism through a one-photon process. Of his observed origin transitions, all

[⊗] Abstract published in *Advance ACS Abstracts*, June 15, 1995.

(1) Dieke, G. H.; Duncan, A. B. F. *Spectroscopic Properties of Uranium Compounds*; McGraw-Hill: New York, 1949.
 (2) Engel, G. Z. *Krist.* **1935**, *90*, 341–373.
 (3) Flint, C. D.; Tanner, P. A. *Mol. Phys.* **1987**, *61*, 389–407. Wu, X.; Dai, S.; Toth, L. M.; Peterson, J. R. *Chem. Phys.* **1995**, *193*, 339–344.

(4) Denning, R. G.; Snellgrove, T. R.; Woodward, D. R. *Mol. Phys.* **1975**, *30*, 1819–1828.

(5) Denning, R. G.; Snellgrove, T. R.; Woodward, D. R. *Mol. Phys.* **1976**, *32*, 419–442.

(6) Flint, C. D.; Tanner, P. A. *J. Chem. Soc., Faraday Trans. 2* **1978**, *74*, 2210–2217.

(7) Watkin, D. J.; Denning, R. G.; Prout, K. *Acta Crystallogr.* **1991**, *C47*, 2517–2519.

Table 1. Vibronic Structure and Assignments (ν in cm^{-1}) for the Luminescence of $\text{UO}_2\text{Cl}_4^{2-}$ in $\text{Cs}_2\text{UO}_2\text{Cl}_4$ and in $\text{Cs}_2\text{ZrCl}_6:\text{UO}_2\text{Cl}_4^{2-}$ at 20 K^a

$\text{Cs}_2\text{UO}_2\text{Cl}_4^b$	$\text{Cs}_2\text{ZrCl}_6:\text{UO}_2\text{Cl}_4^{2-}$	mode ^c	sym (D_{4h})	vibration
108, 117	116	ν_{10}	b_{1u}	O–U–Cl out of plane bend
246	247	ν_3	e_u	O–U–O bend
831	819	ν_1	a_{1g}	O–U–O sym stretch
916	901	ν_2	a_{2u}	O–U–O asym stretch

^a Assignments of vibronic structure based on origins of 20 095.7 and 20 097.3 cm^{-1} for $\text{Cs}_2\text{UO}_2\text{Cl}_4$ and of 19 692 cm^{-1} for $\text{Cs}_2\text{ZrCl}_6:\text{UO}_2\text{Cl}_4^{2-}$. ^b From ref 6. ^c Notation from ref 5.

except one are allowed by a magnetic-dipole mechanism. The exception is allowed by an electric-quadrupole mechanism.⁴ Five of the origin transitions are not observed but are assigned based on associated vibronic progressions. There are transitions that show polarization properties consistent with a electric-dipole mechanism, but they are all vibronic transitions based on electric-dipole forbidden origins. Magnetic-dipole allowed vibronic transitions are observed which are based on magnetic-dipole allowed origins coupled with the symmetric stretching mode of the UO_2^{2+} ion.

In a subsequent study, Denning and co-workers⁸ verified the existence and location of four of the five electric-dipole forbidden origin transitions through the use of two-photon spectroscopy and found two additional origins higher in energy. The complementary nature of the one- and two-photon measurements on this system ensures that the observed electronic origins in the 20 000–30 000 cm^{-1} region are well characterized and gives strong support for Denning's assignments of the electronic structure of the UO_2^{2+} ion in $\text{Cs}_2\text{UO}_2\text{Cl}_4$.

Flint and Tanner⁶ analyzed the luminescence spectra of $\text{Cs}_2\text{UO}_2\text{Cl}_4$ at 20 K on the basis of Denning's analysis of the electronic and vibronic structure of the compound. Luminescence is observed from the lowest excited state origins of Π_g ($D_{\infty h}$) parentage at 20 095.7 and 20 097.3 cm^{-1} . The vibronic structure associated with these origins reflects the ground-state vibrational structure of the uranyl ion. Denning⁵ had assigned the normal mode vibrations of $\text{UO}_2\text{Cl}_4^{2-}$ in $\text{Cs}_2\text{UO}_2\text{Cl}_4$ on the basis of previous infrared⁹ and Raman spectra, and Flint and Tanner used these assignments in their analysis of the luminescence spectra. The strongest vibronic bands are associated with the O–U–Cl bending mode (ν_{10} in Denning's notation⁵), the O–U–O bending mode (ν_3), the O–U–O symmetric stretch (ν_1), and the O–U–O asymmetric stretch (ν_2). Flint and Tanner's assignments of the observed luminescence vibronic structure are given in the first column of Table 1.

Experimental Section

The Cs_2ZrCl_6 host crystal is hygroscopic, so care must be taken in its preparation and handling in order to prevent contamination by moisture. The UO_2Cl_2 starting material was prepared by the method given in the literature.¹⁰ The compound $\text{Cs}_2\text{UO}_2\text{Cl}_4$ was synthesized by melting a stoichiometric mixture of CsCl and UO_2Cl_2 at 850 °C. Crystals of Cs_2ZrCl_6 doped with $\text{UO}_2\text{Cl}_4^{2-}$ were grown by the Bridgman technique from melts at 850 °C containing a stoichiometric mixture of ZrCl_4 and CsCl with 1 mol % $\text{Cs}_2\text{UO}_2\text{Cl}_4$.

Crystals from the solidified melt were polished using filter paper and methanol and mounted using indium foil and Crycon grease to the

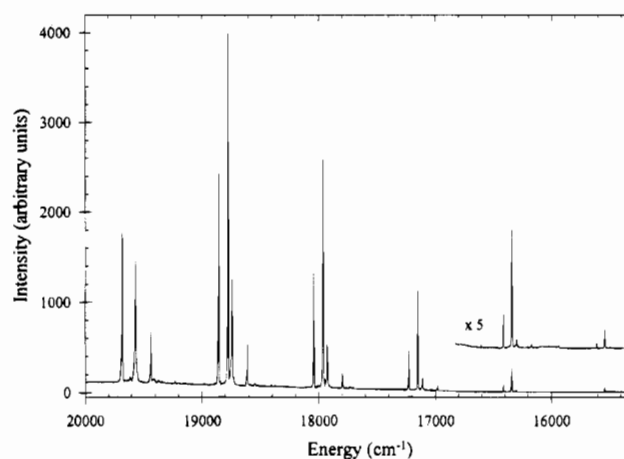


Figure 1. Survey emission spectrum for a single crystal of $\text{Cs}_2\text{ZrCl}_6:\text{UO}_2\text{Cl}_4^{2-}$ at 20 K. This spectral range covers the true and false origin lines of the $A_{1g} \leftarrow E_g$ electronic origin transition and the first five members of the UO_2^{2+} symmetric stretching mode. The excitation wavelength was 465.8 nm.

one-piece copper optical mount of a ADP DE-202 closed-cycle helium refrigerator. The temperature of the copper mount was monitored with a silicon diode temperature sensor mounted directly above the crystal. We estimate the crystal temperature to be within 5 K of the sensor temperature reading.

Luminescence from the crystal was excited with the 457 or 465 nm line of a Spectra-Physics Model 165 argon ion laser. Excitation power was ca. 50 mW at the sample. Fiberoptics were used in both the excitation and emission optical pathways to and from the sample. The emission was collected at 180° with respect to the excitation direction, and dispersed with a Spex 500M monochromator with a 1200 groove/mm grating blazed at 500 nm. The dispersed radiation was detected using a CCD detector (Spex System One) with a 1 in. CCD chip. The resolution limit of this system is determined by the dispersion of the grating, the focal length of the monochromator, and the pixel size of the CCD detector and is 0.04 nm. Entrance slit widths less than 20 μm provide this resolution and were used in these measurements. Emission spectra were corrected for the wavelength-dependent intensity response characteristics of our monochromator-detector system by dividing the spectra by a set of correction factors generated by measuring the instrumental response to a tungsten light source of known spectral characteristics. No attempt was made to determine absolute emission intensities for this system.

Results

Spectra. A survey emission spectrum for a single crystal of Cs_2ZrCl_6 doped with ca. 1% $\text{UO}_2\text{Cl}_4^{2-}$ held at a temperature of 20 K is shown in Figure 1. The spectral range shown (20 000–15 300 cm^{-1}) spans the true and false origin lines of the $A_{1g} \leftarrow E_g$ electronic transition region of the UO_2^{2+} ion ($\Sigma_g^+ \leftarrow \Pi_g$ in the $D_{\infty h}$ point group) and the first five members of vibronic progressions in the symmetric stretching frequency of the UO_2^{2+} ion based on these origins. The false origin lines are displaced from the true electronic origin (or zero-phonon line) at 19 692 cm^{-1} by the frequencies of the nonsymmetric vibrational modes of the UO_2^{2+} ion listed in Table 1.

The false-origin lines are *non-Franck–Condon allowed* transitions, because the vibrational modes associated with these transitions cannot induce the coordinate change necessary to reach the ground-state equilibrium structure of the UO_2^{2+} ion after it undergoes a (vertical) transition from its excited state. However, these lines can serve as origins for *Franck–Condon allowed* progressions in the symmetric stretching frequency (ν_1 , at 819 cm^{-1}), since this vibration can induce the necessary geometry change along the uranyl bond length coordinate between excited state and ground state UO_2^{2+} . This is why they are termed “false-origin lines”.

(8) Barker, T. J.; Denning, R. G.; Thorne, J. R. G. *Inorg. Chem.* **1987**, *26*, 1721–1732.

(9) Ohwada, K. *Spectrochim. Acta* **1975**, *A31*, 973–977.

(10) Leary, J. A.; Suttle, J. F. *Inorg. Synth.* **1957**, *5*, 148–150.

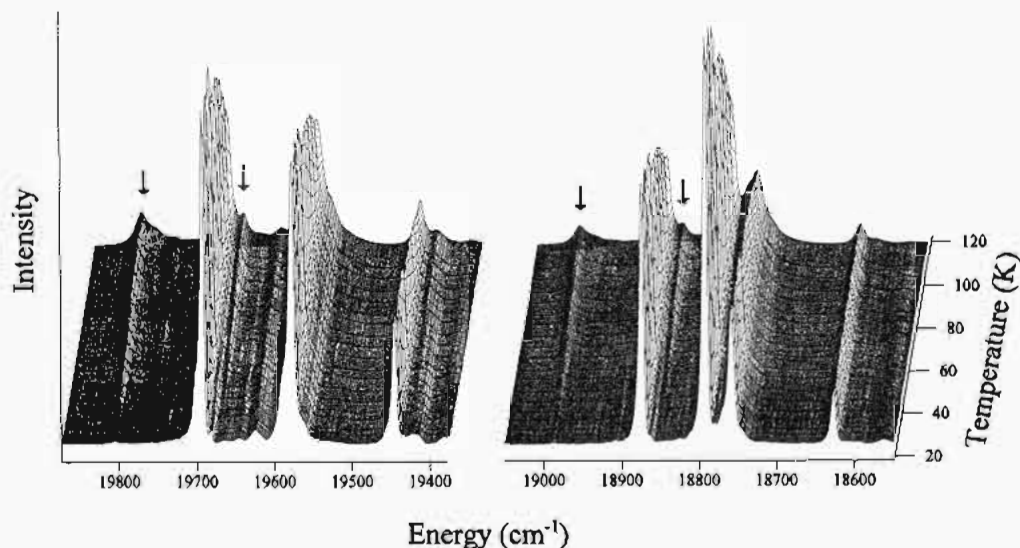


Figure 2. Emission spectra of the true and false origin region (left) and members of the first vibronic progression region (right) taken as a function of temperature. The intensity range of the right region has been scaled by 50%. The arrows point to hot false origin transitions (left) and the first members of progressions based on these false origins (right). See text for details.

Figure 2 shows spectra spanning the true and false origin region and the members of the first vibronic progression as a function of temperature. All of the transitions show a broadening as the temperature is increased (with a concurrent decrease in their peak heights). The positions of the transitions also show a slight shift to higher energy as the temperature is increased. This shift (for all of the transitions) is about 10 cm⁻¹ as the temperature is increased from 20 to 125 K. Of interest in these spectra is the appearance of two hot false origin transitions at 19 807 and 19 674 cm⁻¹, as indicated by the two arrows in the origin region of the figure. These two bands serve as origins for progressions in the symmetric stretching mode of the uranyl ion, and members of these progressions are seen on into the low-energy portions of the emission spectra at temperatures above 20 K. The two right-most arrows in Figure 2 indicate the first members of the progressions based on these two hot origins.

The high-energy hot origin (at 19 807 cm⁻¹) is associated with thermal population of a vibronic level above the emission origin electronic state. The vibration associated with this level is the *excited-state* O–U–Cl bending mode, which we denote by ν_{10}^* . On the basis of these spectra, this vibrational frequency is 114 cm⁻¹. The frequency of this vibration in the *ground state* (ν_{10}) is 116 cm⁻¹. The intensity of the second hot origin (at 19 674 cm⁻¹) appears to have the same dependence on temperature as that of the first hot origin. It is tempting to assign the second origin to a vibronic transition involving two phonons of the same vibrational mode: one in the excited state and one in the ground state. The frequency of this transition would be $E + \nu_{10}^* - \nu_{10}$, where E denotes the energy of the true electronic origin (19 692 cm⁻¹). However, the expected frequency of this transition would nearly coincide with that of the true electronic origin (E), whereas the observed transition occurs some 20 cm⁻¹ to the low-energy side of the electronic origin. At present, we are unable to assign this second hot origin.

Vibronic Intensity Calculations. As noted above, lines coupled to the true electronic origin (zero-phonon line) by one vibrational quanta in a nonsymmetric mode serve as origins for progressions in the symmetric stretching mode of the UO₂²⁺ ion. The intensity distributions observed for progressions associated with the E true origin and with each $E - \nu_a$ false origin were used to determine Huang–Rhys parameters for the

A_{1g} ground state and E_g excited state. Here, ν_a denotes one of the nonsymmetric modes listed in Table 1 (ν_{10} , ν_3 , or ν_2). In our analysis, the intensity of a vibronic transition relative to that of its origin transition is related to the ratio of the Franck–Condon overlap factors for the transitions

$$\frac{I_{n,0}}{I_{0,0}} = \left(\frac{E - \nu_a - n\nu_1}{E - \nu_a} \right)^4 \left(\frac{\langle n|0\rangle}{\langle 0|0\rangle} \right)^2 \quad (1)$$

Here $I_{n,0}$ denotes the intensity of the transition from the 0th vibrational level of the excited state to the n th vibrational level of the ground state, E is the energy of the true electronic origin (as before, 19 692 cm⁻¹), ν_a is the frequency of a nonsymmetric vibrational mode listed in Table 1 (or zero, for the progression based on the true origin), and ν_1 is the UO₂²⁺ symmetric stretching frequency (819 cm⁻¹). The overlap integrals are calculated using the Manneback recursion formulas¹¹ in notation modified by Fonger and Struck:^{12,13}

$$\langle 0|0\rangle = \sin^{1/2} 2\theta \exp(-1/8 \sin^2 2\theta a_{uv}^2) \quad (2)$$

$$\langle n+1|0\rangle = (n+1)^{-1/2} (\cos 2\theta n^{1/2} \langle n-1|0\rangle + \sin 2\theta 2^{-1/2} a_{uv} \sin \theta \langle n|0\rangle) \quad (3)$$

In these equations, the angle θ is defined in terms of the angular frequencies of the symmetric stretching mode in the ground (u) and excited (v) states:

$$\theta = \tan^{-1} \left(\frac{\omega_v}{\omega_u} \right)^{1/2} \quad (4)$$

The dimensionless offset parameter a_{uv} can be related to the Huang–Rhys parameters for the ground (u) and excited (v) states:

$$S_u^{1/2} = 2^{-1/2} a_{uv} \cos \theta \quad S_v^{1/2} = 2^{-1/2} a_{uv} \sin \theta \quad (5)$$

The Huang–Rhys parameters in turn can be related to the offset

- (11) Manneback, C. *Physica* **1951**, *17*, 1001.
- (12) Fonger, W. H.; Struck, C. W. *J. Chem. Phys.* **1974**, *60*, 1994–2002; Struck, C. W.; Fonger, W. H. *J. Luminesc.* **1975**, *10*, 1–30.
- (13) The recursion formulas in ref 12 allow for calculation of overlap integrals of the form $\langle n|m\rangle$, where m refers to the m th vibrational level of the initial state. As we are only interested in the $\langle n|0\rangle$ integrals (there is negligible thermal population of $m > 0$ levels at 20 K), we have simplified the formulas accordingly.

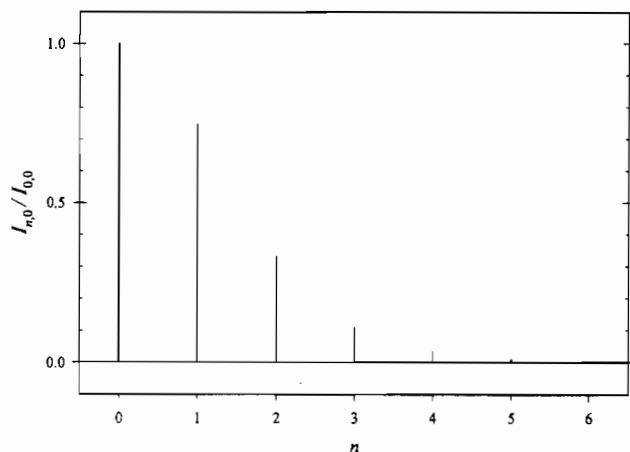


Figure 3. Emission intensity distribution calculated for a progression in the UO_2^{2+} symmetric stretching mode. See text for details.

(in units of length) between the electronic states:

$$x = \left[\frac{2S_e \hbar}{\omega_e M} \right]^{1/2} \quad (6)$$

Here, S_e and ω_e are the Huang–Rhys parameter and symmetric stretch angular frequency for either the ground or excited states ($Q = u$ or v) and M is the effective mass. The offset x represents the length difference along the symmetric stretching coordinate between the minima of the parabolas representing the ground and excited states. For UO_2^{2+} , this represents the difference in U–O bond lengths of the two states.

In all of the above, we assume that emission only occurs from the 0th vibrational level of the excited state. We use values of 819 and 693 cm^{-1} for the ground- and excited-state symmetric stretching frequencies for UO_2^{2+} doped in Cs_2ZrCl_6 . (The latter value is taken from absorption measurements on this system.) Fits of the experimental intensity data to eqs 2 and 3 lead to a value of a_{uv} , which in turn, leads to values of 1.05 and 0.89 for the Huang–Rhys parameters for the ground (A_{1g}) and excited (E_g) states, respectively. These correspond to a U–O bond length difference of ca. 7.3 pm between the ground and excited states. Figure 3 shows relative intensities expected for a progression in the symmetric stretching mode, calculated using eqs 1–3. The calculated intensity distribution closely matches those seen in Figure 1 when self-absorption in the true electronic origin transition (which lowers the observed emission intensity in this line) is taken into account.

The intensity pattern observed for the vibronic progressions of the UO_2^{2+} ion in this lattice is similar to that seen for the UO_2^{2+} ion in other crystalline systems, and by implication, the degree of bond lengthening calculated is typical for uranyl systems. There are a few reports of Huang–Rhys calculations (of varying rigor) on uranyl systems that have appeared in the literature;¹⁴ this result is consistent with those.

Discussion

Emission spectra of crystalline uranyl compounds at low temperatures generally consist of progressions of sharp lines based on true origins and vibronically allowed false origins. The emission origin (the zero-phonon true origin) is assigned to the Σ_g^+ (σ_u^2) \leftarrow Π_g ($\sigma_u \delta_u$) transition (where the molecular orbital occupancy is given). This transition involves the movement of an electron from a nonbonding orbital (δ_u) to a

bonding orbital (σ_u) of the uranyl ion. The energy of this transition will be related to the strength of the U–O bond, as will be the spacings of lines coupled to the origin via vibrations associated with the U–O bond. Denning, in his recent review of electronic structure and bonding in actinyl ions,¹⁵ has published a correlation between U–O bond length and first electronic excited state energy, and Bartlett and Cooney¹⁶ have obtained an empirical formula expressing the U–O bond length (in pm) in terms of the symmetric stretching frequency:

$$R_{\text{U-O}} = (10650 \nu_1^{-2/3}) + 57.5 \quad (7)$$

The perturbing influence on the U–O bond is the coordination of equatorial ligands to the UO_2^{2+} . There is a rough charge relationship: the more negative the equatorial ligand atoms, the weaker the U–O bond, the lower the first excited state energy, and the lower the symmetric stretching frequency.

In our present system, the energy of the electronic origin is 19,692 cm^{-1} . This is toward the low-energy end of the range of first excited state energies compiled by Denning,¹⁵ and suggests a weakening of the U–O bond strength as a result of the equatorial chloride ligand coordination in $\text{UO}_2\text{Cl}_4^{2-}$ doped Cs_2ZrCl_6 . On the other hand, the electronic origin for $\text{UO}_2\text{Cl}_4^{2-}$ in neat $\text{Cs}_2\text{UO}_2\text{Cl}_4$ occurs at 20 096 cm^{-1} ,⁵ which is in the middle of the range of first excited-state energies. Thus, doping of $\text{UO}_2\text{Cl}_4^{2-}$ in the Cs_2ZrCl_6 lattice results in a decrease of the energy of the origin transition of some 400 cm^{-1} . The effect on vibrational frequencies is less pronounced, with a decrease in the UO_2^{2+} symmetric stretching frequency of 12 cm^{-1} (see Table 1). Application of eq 7 to the symmetric stretch frequency data listed in Table 1 predicts a ground-state U–O bond lengthening of less than 1% in the Cs_2ZrCl_6 lattice as compared to the neat system.

There are a number of factors that can affect the relative energies of the ground and excited states of the uranyl ion in these systems. A structural effect of doping $\text{UO}_2\text{Cl}_4^{2-}$ in the Cs_2ZrCl_6 lattice is a compression of the U–Cl bond length, as compared to the bond length in the neat $\text{Cs}_2\text{UO}_2\text{Cl}_4$ crystal. In Cs_2ZrCl_6 , the Zr–Cl bond length is 245 pm,² and in $\text{Cs}_2\text{UO}_2\text{Cl}_4$, the U–Cl bond length is 267 pm.⁷ Doping of the $\text{UO}_2\text{Cl}_4^{2-}$ ion in a ZrCl_6^{2-} site thus results in a U–Cl bond compression of 22 pm. This compression is expected to increase the energies of both the σ_u HOMO (the highest occupied molecular orbital) as well as the δ_u LUMO (the lowest unoccupied molecular orbital), since both orbitals are thought to be largely uranium 5f in character. A prediction of the net effect of the U–Cl bond compression on the magnitude of the energy gap between the HOMO and LUMO is difficult.

A further lattice effect on the molecular orbitals of the $\text{UO}_2\text{Cl}_4^{2-}$ ion is the charge potential of the Cs ions and their position relative to the uranyl oxygen atom. In the $\text{Cs}_2\text{UO}_2\text{Cl}_4$ lattice, the oxygen atom has three Cs cation neighbors, one of which is located almost directly on the uranyl bond axis, 332 pm from the oxygen.⁷ In the Cs_2ZrCl_6 lattice, the dopant $\text{UO}_2\text{Cl}_4^{2-}$ ion has its uranyl oxygen atom located slightly below the center of a square of four Cs cations, with an estimated Cs–O distance of 376 pm. The effect of an axially proximate positive ion (in the $\text{Cs}_2\text{UO}_2\text{Cl}_4$ system) would be to lower the energy of the oxygen 2p_σ orbital which is directed along the U–O bond, thus lowering the energy of the HOMO and increasing the size of the HOMO–LUMO gap. This may explain the higher excitation energies observed in $\text{Cs}_2\text{UO}_2\text{Cl}_4$ as compared to $\text{Cs}_2\text{ZrCl}_6:\text{UO}_2\text{Cl}_4^{2-}$.

(14) Denning, R. G. In *Vibronic Processes in Inorganic Chemistry*; NATO ASI Series C: Mathematical and Physical Sciences 288; Flint, C. D., Ed.; Kluwer Academic Publishers: Dordrecht, The Netherlands, 1989; pp 111–137. Moran, D. M.; Metcalf, D. H.; Richardson, F. S. *Inorg. Chem.* **1992**, *31*, 819–825.

(15) Denning, R. G. *Struct. Bonding* **1992**, *79*, 215–276.

(16) Bartlett, J. R.; Cooney, R. P. *J. Mol. Struct.* **1989**, *193*, 295–300.

Conclusion

In this study, we have examined in detail the luminescence of crystals of the doped system $\text{Cs}_2\text{ZrCl}_6:\text{UO}_2\text{Cl}_4^{2-}$ at low temperatures, with emphasis on the correlation of the spectra with uranyl electronic and physical structure. The luminescence vibronic structure is fully consistent with the dopant uranyl ion being at a site of exact D_{4h} symmetry, and the distribution of vibronic intensity among members of progressions based on the symmetric stretching mode is consistent with a uranyl bond lengthening of ca. 4% on excitation to the emitting state. An unusual feature of the spectrum, that of the low energy of the electronic origin of the luminescence (as compared to the neat crystal $\text{Cs}_2\text{UO}_2\text{Cl}_4$), can be explained in terms of changes in the Coulombic field experienced by the $\text{UO}_2\text{Cl}_4^{2-}$ ion as it is accommodated in the Cs_2ZrCl_6 lattice.

As is noted in the Introduction, there is an extensive series of hexahalide compounds that crystallize in the hexachloroplatinate structure. We are continuing our spectral characterization of uranyl ion doped in members of this series, to examine the effects on the vibronic and electronic structures of the UO_2^{2+} ion as we systematically tune the lattice.

Acknowledgment. This work was supported by the U.S. Department of Energy, Office of Basic Energy Sciences, under Contract DE-AC05-84OR21400 with Martin Marietta Energy Systems. We also thank a reviewer for valuable comments regarding lattice geometry effects on the electronic structure of the $\text{UO}_2\text{Cl}_4^{2-}$ ion.

IC950111C